Quaternion Angular Radial Transform and Properties Transformation for Color-Based Object Recognition[1]

A. Khatabi[a]*, A. Tmiri[a], and A. Serhir[b]*****

[a] *Dept. of Computer Science, Chouaib Doukkali University El Jadida, Morocco*
[b] *Dept. of Math, Chouaib Doukkali University El Jadida, Morocco*
*e-mail: *khatabiabdo5@gmail.com, **B_tmiri@yahoo.fr, ***A.serhir@gmail.com*

Abstract—Nowadays, with the increased use of digital images, almost all of which are in color format. Conventional methods process color images by converting them into gray scale, which is definitely not effective in representing and which may lose some significant color information. Recently, a novel method of the Color Angular Radial Transform (CART) is presented. This transform combines the information by considering the shape information inherent in the color. However, ART is adapted on the MPEG-7 standard is only limited to binary images and gray-scale images has many properties: invariant to rotation, Translation and scaling, ability to describe complex objects, so it cannot handle color images directly. To solve this problem we proposed in this article to generalize ART from complex domain to hypercomplex domain using quaternion algebras to achieve the Quaternion Angular Radial Transform (QART) to describe finally two dimensional color images and to insure these properties robustness to all possible rotations and translation and scaling. The performance of QART is then evaluated with large database of color image as an example. We first provide a general formula of ART from which we derive a set of quaternion-valued QART properties transformations by eliminating the influence of transformation parameters. The experimental results show that the QART performs better than the commonly used Quaternion form Zernike Moment (QZM) in terms of image representation capability and numerical stability.

Keywords: color image, ART descriptor, quaternion, quaternion angular radial transform recognition
DOI: 10.1134/S1054661816040064

1. INTRODUCTION

Nowadays, ease of accessibility of digital photographic devices gives rise to the use of color images. Color images contain more appearance information and provide more accurate descriptions of real-world objects than grey-scaled images [1, 2]. The inefficient conventional methods for image processing typically involve the conversion of color images to gray scale images, causing loss in significant color information. To address this problem, quaternion theory have been presented into color image processing such as image watermarking [3], sparse representation [4], image quality assessment [5], and image authentication [6]. Quaternion-based moment functions have also recently been applied for image processing of color images [7–9] and [10].

Quaternion model have gained popularity for application in color image processing to represent color images by decomposing three channels into the imaginary parts of quaternion numbers [11]. This can be viewed as the generation of traditional complex number which was introduced by Hamilton in 1843 [12].

Quaternion representation advantageously treats color images holistically as a vector field [13], as proposed by Sangwine [14, 15], where it involves combination of a color 3-tuple (RGB) into a single hypercomplex number. Examples include the application of Quaternion Gabor Filter (QGF) [16] and quaternion Fourier transforms [17] to estimate motion and color image registration [18], dual-tree quaternion wavelets for multiscale image processing [19], wavelet transform [20], independent component analysis, singular value decomposition, and Clifford-Fourier transform for color image processing [21], and polar harmonic transform [22].

Orthogonal moments/transforms have been widely used in image analysis, such as data hiding [23], visual quality assessment [24] and vision computer, where the Angular Radial Transform (ART) is a moment based image description method adopted in MPEG-7 as a region based shape descriptor [25]. It gives a compact and efficient way to express pixel distribution within a 2D object region; it can describe both connected and disconnected region shapes.

This paper reports the extension of conventional ART to allow the handling of color images in a holistic manner. To accomplish this, algebra of quaternions, which have gained popularity for applications in color image processing in recent years, will be utilized.

[1]The article is published in the original.

Received February 10, 2016

The RGB image can be represented by decomposing three channels red, green and blue components of the pixel.

The advantage this provides is it encodes three channels into the imaginary parts of quaternion numbers of color images. The algebra of quaternions has been proposed in color image processing by Ell and Sangwine [26]. Ell introduced the quaternion Fourier transforms (QFTs) in 1992 [27]. Later Sangwine applied QFTs for use in color images.

In this paper we focus on properties under Angular Radial Transform to extend the conventional moments to color image processing and we introduce a generalization of the ART for color images using Quaternion algebra.

Quaternion Angular Radial Transform (QART) with respect to properties transformations is presented. The performance of QART was then evaluated with large database of Wang's color images. QART was also compared to Quaternion form Zernike Moment (QZM) for its efficiency, precision and recall.

There meaning of this paper is organized as follows. Preliminaries of the quaternions will be recalled and its color representation will be defined in Section 2. The derivation of coefficients of ART with respect to transformations of properties such as invariant to rotation, scale and translation of QART will be shown in Section 3. Experimental results are provided in Section 4 to illustrate the performance of the proposed descriptor and Section 5 concludes the paper.

2. QUATERNION ANGULAR RADIAL TRANSFORM

2.1. Quaternion Color Representation

Quaternions, introduced by the mathematician Hamilton [28] in 1843, are generalizations of complex numbers. A quaternion has one real part and three imaginary parts given by

$$q = a + bi + cj + dk, \tag{1}$$

where a, b, c, d are real numbers, and i, j, k are three imaginary units obeying the following rules

$$i^2 = j^2 = k^2 = -1, \tag{2}$$

$$ij = -ij = k, \quad jk = -kj = i, \quad ki = -ik = j. \tag{3}$$

If the real part $a = 0$, q is called a pure quaternion. The conjugate and modulus of a quaternion are respectively defined by

$$q^* = a - bi - cj - dk, \tag{4}$$

$$\|q\| = \sqrt{a^2 + b^2 + c^2 + d^2}. \tag{5}$$

Let $f(x, y)$ be an RGB image function with the quaternion representation. Each pixel can be represented as a pure quaternion

$$f(x,y) = f_R(x,y)i + f_G(x,y)j + f_B(x,y)k, \tag{6}$$

where $f_R(x, y), f_G(x, y)$, and $f_B(x, y)$ are respectively the red, green and blue components of the pixel.

2.2. Angular Radial Transform

ART is a complex orthogonal unitary transform defined on a unit disk based on complex orthogonal sinusoidal basis functions in polar co-ordinates [29–31]. The ART coefficients, F_{nm} of order n and m, are defined by:

$$F_{nm} = \int_0^{2\pi}\int_0^1 V^*_{nm}(r,\theta) f(r,\theta) r dr d\theta, \tag{7}$$

where $f(r, \theta)$ is an image intensity function in polar coordinates and $V^*_{nm}(r, \theta)$ is a basis function, which is complex conjugate of $V_{nm}(r, \theta)$ defined in polar coordinates over a unit disk. These are expressed in a separable form of both radial and angular parts as follows:

$$V_{nm}(\rho,\theta) = A_m(\theta)R_n(\rho). \tag{8}$$

The indices n and m are non-negative integers. The real valued radial polynomial and the angular basis function are defines as:

$$R_n(r) = \begin{cases} 1 & n = 0, \\ 2\cos(\pi n\rho) & n \neq 0. \end{cases} \tag{9}$$

$$A_m(\theta) = \frac{1}{2\pi}\exp(jm\theta), \tag{10}$$

Where $j = \sqrt{-1}$ the important characteristics of ART is the rotational invariance. The original image is represented by the intensity image function $f(r, \theta)$ having ART is rotated counterclockwise by angle α; the transformed image function is

$$g(r,\theta) = f(r,\theta - \alpha). \tag{11}$$

The ART coefficients of original and rotated images are F_{nm} and $F^{\text{rot}}_{nm} = e^{-jm\theta}F_{nm}$, the magnitude values are identical, where $\|e^{-jm\theta}\| = 1$.

In [35] shows that if ART coefficients are calculated in the polar coordinate system eliminates the geometric and integral error.

The standard MPEG-7 recommends using 12 features angular and 3 radial functions ($n = 3$ and $m = 12$). The distance measure between two shapes described by ART is obtained by using the L1 norm:

$$D_{ART}(R,M) = \sum_{k=0}^{n.m} \|ART_m[k] - ART_R[k]\|. \tag{12}$$

2.3. Quaternion Angular Radial Transform and Their Properties

In this section, we first define the general formula of QART for color images before constructing a set of quaternion-value of properties (rotation, scale, and

translation (RST) transformations). At last we propose an efficient algorithm that implements QART.

According to the general definition of Angular Radial Transform, and to quaternion algebra, the general formula of the QART of a color image $f(r, \theta)$ an RGB image defined in polar coordinates, the right-side QART of order n with repetition m is introduced as:

$$F_{n,m}^{R} = \frac{1}{2\pi}\int_{0}^{2\pi}\int_{0}^{1} R_n(r) f(r,\theta) e^{-\mu m\theta} r dr d\theta, \tag{13}$$

where μ is a unit pure quaternion chosen as

$$\mu = (i + j + k)/\sqrt{3}. \tag{14}$$

2.3.1. Formula of quaternion angular radial transform. We add the Eq. (6) of quaternion to the Eq. (13) of coefficients becomes ART

$$\begin{aligned}
F_{n,m}^{R} &= \frac{1}{2\pi}\int_{0}^{2\pi}\int_{0}^{1} R_n(r)[f_R(r,\theta) \\
&+ f_G(r,\theta) + f_B(r,\theta)]e^{-\mu m\theta} r dr d\theta, \\
F_{n,m}^{R} &= i\frac{1}{2\pi}\int_{0}^{1}\int_{0}^{2\pi} R_n(r) f_R(r,\theta) e^{-\mu m\theta} r dr d\theta \\
&+ j\frac{1}{2\pi}\int_{0}^{1}\int_{0}^{2\pi} R_n(r) f_G(r,\theta) e^{-\mu m\theta} r dr d\theta \\
&+ k\frac{1}{2\pi}\int_{0}^{1}\int_{0}^{2\pi} R_n(r) f_B(r,\theta) e^{-\mu m\theta} r dr d\theta.
\end{aligned}$$

According to Euler, we should regard the complex exponential as related to the trigonometric functions $\cos(m\theta)$ and $\sin(m\theta)$ via the following inspired definition:

$$\begin{aligned}
e^{-\mu m\theta} &= \cos(m\theta) - \mu\sin(m\theta) \\
\text{and} \qquad e^{\mu m\theta} &= \cos(m\theta) + \mu\sin(m\theta).
\end{aligned}$$

The coefficients ART becomes:

$$\begin{aligned}
F_{n,m}^{R} &= i\frac{1}{2\pi}\int_{0}^{1}\int_{0}^{2\pi} R_n(r) f_R(r,\theta)[\cos(m\theta) - \mu\sin(m\theta)] r dr d\theta \\
&+ j\frac{1}{2\pi}\int_{0}^{1}\int_{0}^{2\pi} R_n(r) f_G(r,\theta)[\cos(m\theta) - \mu\sin(m\theta)] r dr d\theta \\
&+ k\frac{1}{2\pi}\int_{0}^{1}\int_{0}^{2\pi} R_n(r) f_B(r,\theta)[\cos(m\theta) - \mu\sin(m\theta)] r dr d\theta.
\end{aligned}$$

$$\begin{aligned}
F_{n,m}^{R} &= i\left[\frac{1}{2\pi}\int_{0}^{1}\int_{0}^{2\pi} R_n(r) f_R(r,\theta)\cos(m\theta) r dr d\theta\right. \\
&\left. - \mu\frac{1}{2\pi}\int_{0}^{1}\int_{0}^{2\pi} R_n(r) f_R(r,\theta)\sin(m\theta) r dr d\theta\right] \\
&+ j\left[\frac{1}{2\pi}\int_{0}^{1}\int_{0}^{2\pi} R_n(r) f_G(r,\theta)\cos(m\theta) r dr d\theta\right. \\
&\left. - \mu\frac{1}{2\pi}\int_{0}^{1}\int_{0}^{2\pi} R_n(r) f_G(r,\theta)\sin(m\theta) r dr d\theta\right] \\
&+ k\left[\frac{1}{2\pi}\int_{0}^{1}\int_{0}^{2\pi} R_n(r) f_B(r,\theta)\cos(m\theta) r dr d\theta\right. \\
&\left. - \mu\frac{1}{2\pi}\int_{0}^{1}\int_{0}^{2\pi} R_n(r) f_B(r,\theta)\sin(m\theta) r dr d\theta\right].
\end{aligned}$$

The terms of its real and imaginary parts

$$\begin{aligned}
F_{n,m}^{R} &= i\left[\mathrm{Re}(F_{n,m}(f_R)) + \left(\frac{i+j+k}{\sqrt{3}}\right)\mathrm{Im}(F_{n,m}(f_R))\right] \\
&+ j\left[\mathrm{Re}(F_{n,m}(f_G)) + \left(\frac{i+j+k}{\sqrt{3}}\right)\mathrm{Im}(F_{n,m}(f_G))\right] \\
&+ k\left[\mathrm{Re}(F_{n,m}(f_B)) + \left(\frac{i+j+k}{\sqrt{3}}\right)\mathrm{Im}(F_{n,m}(f_B))\right].
\end{aligned}$$

Finally, the quaternion Angular radial Transform is follow:

$$F_{n,m}^{R} = A_{n,m}^{R} + iB_{n,m}^{R} + jC_{n,m}^{R} + kD_{n,m}^{R}, \tag{15}$$

where

$$\begin{aligned}
A_{n,m}^{R} &= -\frac{1}{\sqrt{3}}[\mathrm{Im}(F_{n,m}(f_R)) \\
&+ \mathrm{Im}(F_{n,m}(f_G)) + \mathrm{Im}(F_{n,m}(f_B))], \\
B_{n,m}^{R} &= \mathrm{Re}(F_{n,m}(f_R)) + \frac{1}{\sqrt{3}} \\
&\times[\mathrm{Im}(F_{n,m}(f_G)) - \mathrm{Im}(F_{n,m}(f_B))], \\
C_{n,m}^{R} &= \mathrm{Re}(F_{n,m}(f_G)) + \frac{1}{\sqrt{3}} \\
&\times[\mathrm{Im}(F_{n,m}(f_B)) - \mathrm{Im}(F_{n,m}(f_R))], \\
D_{n,m}^{R} &= \mathrm{Re}(F_{n,m}(f_B)) + \frac{1}{\sqrt{3}} \\
&\times[\mathrm{Im}(F_{n,m}(f_R)) - \mathrm{Im}(F_{n,m}(f_G))],
\end{aligned} \tag{16}$$

where $F_{n,m}(f_R)$, $F_{n,m}(f_G)$ and $F_{n,m}(f_B)$ are respectively the conventional Coefficients ART for the red channel, green channel and blue channel, $\mathrm{Re}(x)$ represents the real part of conventional complex number x, and $\mathrm{Im}(x)$ the imaginary part.

We can define the Left-side QART of order n with repetition m as

$$F^L_{n,m} = A^L_{n,m} + iB^L_{n,m} + jC^L_{n,m} + kD^L_{n,m}, \quad (17)$$

where

$$\begin{aligned} A^L_{n,m} &= -\frac{1}{\sqrt{3}}[\mathrm{Im}(F_{n,m}(f_R)) \\ &+ \mathrm{Im}(F_{n,m}(f_G)) + \mathrm{Im}(F_{n,m}(f_B))], \\ B^L_{n,m} &= \mathrm{Re}(F_{n,m}(f_R)) + \frac{1}{\sqrt{3}} \\ &\times[\mathrm{Im}(F_{n,m}(f_G)) - \mathrm{Im}(F_{n,m}(f_B))], \\ C^L_{n,m} &= \mathrm{Re}(F_{n,m}(f_G)) + \frac{1}{\sqrt{3}} \\ &\times[\mathrm{Im}(F_{n,m}(f_B)) - \mathrm{Im}(F_{n,m}(f_R))], \\ D^L_{n,m} &= \mathrm{Re}(F_{n,m}(f_B)) + \frac{1}{\sqrt{3}} \\ &\times[\mathrm{Im}(F_{n,m}(f_R)) - \mathrm{Im}(F_{n,m}(f_G))]. \end{aligned} \quad (18)$$

2.4. Properties of Quaternion Angular Radial Transform

2.4.1. Rotation invariants. The original image is represented by the intensity image function $f(r, \theta)$ having ART is rotated counter clockwise by angle α; the transformed image function is $g(r, \theta) = f(r, \theta - \alpha)$.

$$\begin{aligned} F^R_{n,m}(f') &= \frac{1}{2\pi}\int_0^{2\pi}\int_0^1 R_n(r)f'(r,\theta)e^{-\mu m\theta}rdrd\theta \\ &= \frac{1}{2\pi}\int_0^{2\pi}\int_0^1 R_n(r)f(r,\theta-\alpha)e^{-\mu m\theta}rdrd\theta \\ &= \frac{1}{2\pi}\int_0^{2\pi}\int_0^1 R_n(r)f(r,\theta)e^{-\mu m(\theta+\alpha)}rdrd\theta \\ &= \frac{1}{2\pi}\int_0^{2\pi}\int_0^1 R_n(r)f(r,\theta)e^{-\mu m\theta}rdrd\theta.e^{-\mu m\alpha} \\ &= F^R_{n,m}e^{-\mu m\alpha}. \end{aligned} \quad (19)$$

The ART coefficients of original and rotated images are $F^R_{n,m}$ and $F^R_{n,m}(f') = e^{-im\alpha}F^R_{n,m}(f)$, the magnitude values are identical, where $\|e^{-im\alpha}\| = 1$.

According in the Eq. (32), we can obtain the following relationship for the left-side QART.

$$F^L_{n,m}(f') = F^L_{n,m}e^{-\mu m\alpha}. \quad (20)$$

Theorem 1. *Let*

$$\begin{aligned} \phi_{n,m}(f) &= F^R_{n,m}(f)F^L_{n,m}(f) \\ &= -F^R_{n,m}(f)(F^R_{n,m}(f))^*. \end{aligned} \quad (21)$$

Then, $\phi_{n,m}(f)$ is invariant to image rotation for any order n and m.

Proof. Let f' be the rotated image of f with rotation angle

$$\begin{aligned} \phi_{n,m}(f') &= F^R_{n,m}(f')F^l_{n,m}(f') = F^R_{n,m}(f)e^{-\mu m\alpha}e^{\mu m\alpha}F^L_{n,m}(f) \\ &= F^R_{n,m}(f)F^L_{n,m}(f) = \phi_{n,m}(f). \end{aligned} \quad (22)$$

The proof has been completed.

2.4.2. Translation invariants. The translation invariance is achieved by considering the center of the polar coordinate system, which is defined as the center of mass of the object, acquired by the geometric moments as follows:

$$\begin{aligned} \bar{Y} &= \frac{(m_{01}(f_R) + m_{01}(f_G) + m_{01}(f_B))}{m_{00}}, \\ \bar{X} &= \frac{(m_{10}(f_R) + m_{10}(f_G) + m_{10}(f_B))}{m_{00}}, \\ m_{00} &= m_{00}(f_R) + m_{00}(f_G) + m_{00}(f_B), \end{aligned} \quad (23)$$

where $m_{00}(f_R)$, $m_{01}(f_R)$, and $m_{10}(f_R)$ are respectively the zero-order and first-order geometric moment for R channel; $m_{00}(f_R)$, $m_{01}(f_G)$ and $m_{10}(f_B)$ are respectively the zero-order and first-order geometric moment for G channel; $m_{00}(f_R)$, $m_{01}(f_D)$, and $m_{10}(f_B)$ are respectively the zero-order and first-order geometric moment for B channel. For discrete channel f_R, f_G, and f_B. The central QART, which are invariant to image translation, can be obtained using the origin of the coordinate system be located at (X, Y) defined as follows

$$F^R_{n,m} = \frac{1}{2\pi}\int_0^1\int_0^{2\pi} R_n(\bar{r})f(\bar{r},\bar{\theta})e^{-\mu m\bar{\theta}}\bar{r}d\bar{r}d\bar{\theta}, \quad (24)$$

where $f(\bar{r}, \bar{\theta})$ the image pixel coordinate representation in polar pixel with mapping transformation using the coordinate $(\bar{X}, \bar{Y})$.

2.4.3. Scaling invariants. For scale invariance, the coefficients of ART are divided by the magnitude of the first coefficient of order $(n = 0, m = 0)$, i.e., by $|F^R_{00}|$

$$\begin{aligned} F^R_{n,m}(f') &= \frac{1}{2\pi}\int_0^1\int_0^{2\pi} R_n(ra)f(ra,\theta)e^{-\mu m\theta}rdrd\theta, \\ F^R_{n,m}(f') &= \frac{1}{2\pi}\int_0^1\int_0^{2\pi} a^2R_n(r)f(r,\theta)e^{-\mu m\theta}rdrd\theta, \\ F^R_{n,m}(f') &= a^2F^R_{n,m}(f), \end{aligned} \quad (25)$$

where $F^R_{n,m}(f')$ and $F^R_{n,m}(f)$ are the QART of $f(ra, \theta)$ and $f(r, \theta)$, respectively.

$$\phi^R_{n,m} = \frac{F^R_{n,m}(f')}{F^R_{0,0}(f')} = \frac{a^2F^R_{n,m}(f)}{a^2F^R_{0,0}(f)} = \frac{F^R_{n,m}(f)}{F^R_{0,0}(f)}. \quad (26)$$

We can construct scale invariants as follows:

$$\phi_{n,m}^{R} = \left\| \frac{F_{n,m}^{R}(f)}{F_{0,0}^{R}(f)} \right\|. \quad (27)$$

When image scaling is concerned, the normalization process is required.

Corollary 1. *The original image is represented by the intensity image function $f(r, \theta)$ having ART is rotated counter clockwise by angle α; the transformed image function is $g(r, \theta) = f(r, \theta - \alpha)$.*

$$F_{n,m}^{R}(f) = F_{n,m}^{R}(f)e^{-\mu m\alpha}.$$

The proof of Corollary 1 is verified.

Corollary 2.

$$\phi_{n,m} = F_{n,m}^{R}(f)(F_{n,m}^{R}(f))^{*}. \quad (28)$$

The proof of Corollary 2 is very similar to that of Theorem 1.

Corollary 3.

$$\overline{\phi}_{n,m}(f) = \overline{F}_{n,m}^{R}(f)(\overline{F}_{n,m}^{R}(f))^{*}, \quad (29)$$

where $\overline{F}_{n,m}^{R}(f)$ is the scaling invariant.

3. CONTENT-BASED COLOR IMAGE RETRIEVAL

3.1. QART Feature Extraction

From the previous calculations, we can obtain rotation, scaling, and translation invariant of QART modulus coefficients. However, the first step in this methodology is to extract the query image features and database of color images. The extraction of different features by descriptor of shape based region ART (angular radial transform) is one of the major stages in designing a reliable image retrieval system.

3.2. Similarity Measure Based on QART Features

Similarity-Based retrieval of images is an important task I many image database applications. After extracting the feature vector, a similarity measurement function is used that measure the similarity between the feature vector of query image and the feature vector of database images.

Euclidean distance (L1 norm) is a straight line distance between any two points and used as a similarity metric.

$$D_E = \sqrt{\sum_{i=0}^{N-1} (A[i] - B[i])^2}, \quad (30)$$

when retrieving color images, we firstly compute the similarity between the query color image and each target color image in the database images using any similarity metrics, and then sort the retrieval results according to the similarity value.

4. EXPERIMENTAL RESULTS

This section is intended to verify the performance of our color image descriptors and the effectiveness of the proposed QART.

The original color image we used is selected from the Columbia University Image Library (COIL-100) and Wang's database.

The experiments have been carried out on a Dual Core PC with 2 GHz CPU and 4 GB memory, within MATLAB 8.1 in Windows. However, the order (n) and repetition (m) we worked with were $n = 3$ and $m = 3$.

4.1. Test the Properties of Proposed Method

4.1.1. Test of rotation invariance. We first test the performance of the QART invariants under rotation transform. The original color image we used was selected from the Columbia University Image Library (COIL-100).

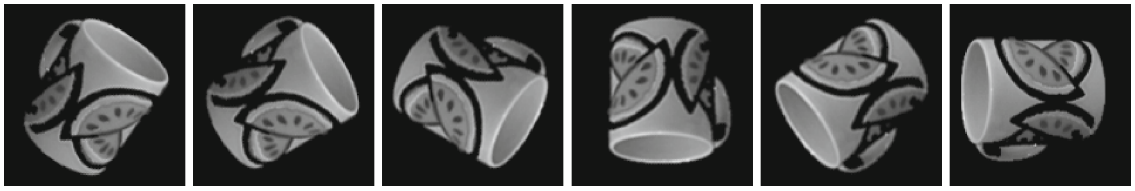

$\alpha = 0°$ $\alpha = 35°$ $\alpha = 60°$ $\alpha = 180°$ $\alpha = 235°$ $\alpha = 270°$

Fig. 1. The original color image and rotation invariance tests.

Table 1. QART invariants rotation of color image

Rotated	$\phi_{1,1}$	$\phi_{2,1}$	$\phi_{3,1}$	$\phi_{1,2}$	$\phi_{2,2}$	$\phi_{3,3}$
$\alpha = 0°$	0.1227	0.2338	0.0125	0.1431	0.1912	0.0134
$\alpha = 35°$	0.1252	0.2366	0.0328	0.1421	0.1931	0.0132
$\alpha = 60°$	0.1242	0.2352	0.0218	0.1462	0.1898	0.0124
$\alpha = 180°$	0.1328	0.2128	0.1513	0.0532	0.0933	0.1214
$\alpha = 235°$	0.1298	0.2336	0.0212	0.1422	0.1942	0.0135
$\alpha = 270°$	0.1244	0.2341	0.0233	0.1487	0.1910	0.0104

Fig. 2. Translation invariance tests.

Table 2. QART invariants translation of color image

Translate	$\phi_{1,1}$	$\phi_{2,1}$	$\phi_{3,1}$	$\phi_{1,2}$	$\phi_{2,2}$	$\phi_{3,3}$
*t*0	0.0889	0.0738	0.0445	0.0504	0.0902	0.0213
*t*1	0.0817	0.0808	0.0098	0.0604	0.0911	0.0211
*t*2	0.0762	0.0532	0.0530	0.0341	0.0878	0.0250
*t*3	0.0602	0.0436	0.0360	0.0890	0.0931	0.0024
*t*4	0.0120	0.0130	0.0603	0.0431	0.0523	0.0621
*t*5	0.0501	0.0425	0.0730	0.0132	0.19001	0.0291

4.1.2. Test of translation invariance. This subsection carried to evaluate the effectiveness of the QART invariants under translation transform. The original color image we used is selected from the Columbia University Image Library (COIL-100).

4.1.3. Test of scale invariance. In this subsection is to evaluate the performance of the QART invariants under scale transform. The original color image we used is selected from the Columbia University Image Library (COIL-100).

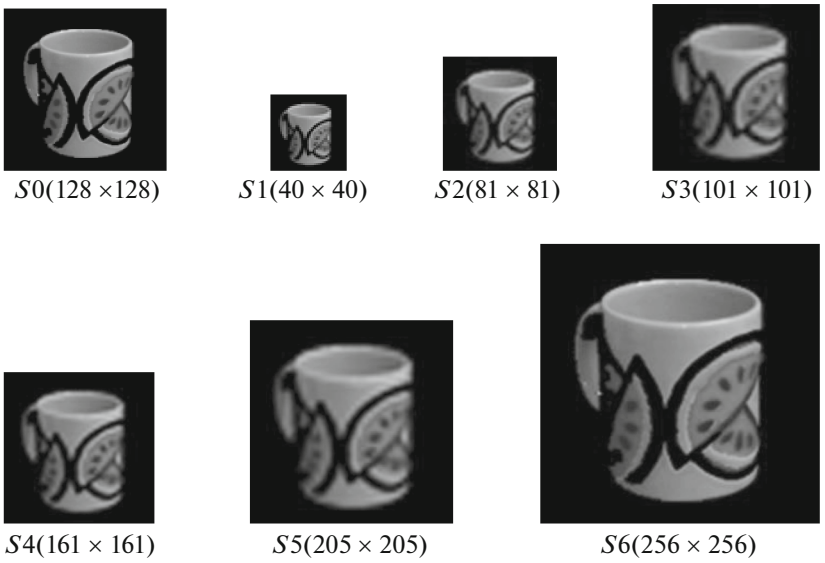

Fig. 3. Scale invariance tests for (COIL-100) image.

Table 3. QART invariants scaling of color image

Scaling	$\phi_{1,1}$	$\phi_{2,1}$	$\phi_{3,1}$	$\phi_{1,2}$	$\phi_{2,2}$	$\phi_{3,3}$
*S*0	0.1912	0.3216	0.1533	0.0023	0.2223	0.1351
*S*1	0.1952	0.3232	0.1548	0.0061	0.2212	0.1354
*S*2	0.1841	0.2241	0.1523	0.0043	0.2240	0.1316
*S*3	0.1945	0.3912	0.0410	0.1204	0.1845	0.0313
*S*4	0.1987	0.3940	0.1593	0.0015	0.2812	0.1252
*S*5	0.1981	0.3890	0.1525	0.0017	0.2919	0.1315
*S*6	0.1931	0.3345	0.1594	0.0116	0.2213	0.1356

Fig. 4. Examples of color images selected from Wang's database.

Fig. 5. The color image retrieval results (Africa) from Wang's database.

4.2. The Performance of QART in Large Database

To evaluate the performance of the proposed QART in a larger database, the sizes of images are 101 × 101 and selected from Wang's color images.

In this section, precision-recall diagrams of Quaternion Angular Radial Transform (QART) and Quaternion Polar complex Exponential Transform (QZM), were constructed.

For high retrieval accuracy, the system needs to have both high precision and high recall rates.

For high retrieval accuracy, the system needs to have both high precision and high recall rates.

$$Recall = (Total\ no.\ of\ Retrieval\ Relevant\ image)/(Total\ no.\ of\ Relevantimage)$$

$$Precision = (Total\ no.\ of\ Retrieval\ Relevantimage)/(Total\ no.\ of\ Retrieval\ image).$$

According to Fig. 6 we found that QART performs better than QZM in image retrieval.

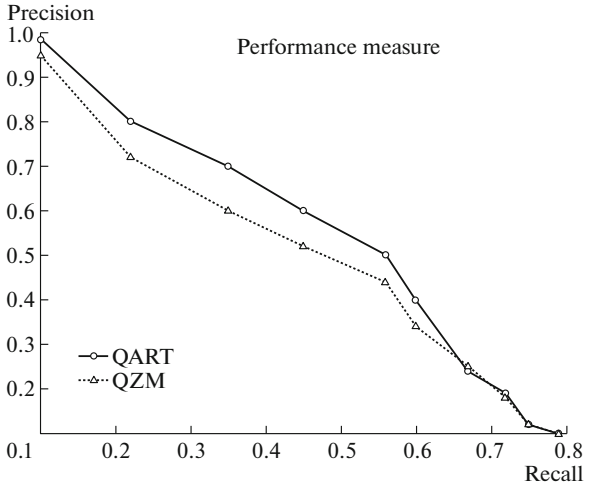

Fig. 6. Precision-recall diagrams of comparison performance between QART and Quaternion form Zernike Moment (QZM).

CONCLUSIONS

Angular Radial Transform (ART) is adapted on binary and gray-scale images, therefore restricting its ability to handle color images directly. To solve this problem, this paper generalizes ART from complex domain to hypercomplex domain using quaternion algebras, producing the Quaternion Angular Radial Transform (QART) for describing color images, and thus the invariance and robustness property of QART was investigated. The results showed that QART perform consistently better in terms of reconstruction error and color image representation capability when examined by Wang's color images, demonstrating that QART is more applicable for processing of color images than conventional ART methods. Precision-recall diagrams of QART and QZM also showed that QART very perform in image retrieval performance when compared to QZM.

ACKNOWLEDGMENTS

We would like to acknowledge the main site where research was carried out; Department of Computer, Chouaib Doukkali University, Faculty of Science, EI Jadida, Morocco.

REFERENCES

1. S. O. Belkasim, M. Shridhar, and M. Ahmadi, "Pattern recognition with moment invariants: a comparative study and new results," Pattern Recogn. **24**, 1117–1138 (1991).
2. Khotanzad and Y. H. Hong, "Invariant image recognition by Zernike moments," IEEE Trans. Pattern Anal. Mach. Intell. **12** (5), 489–497 (1990).
3. T. K. Tsui, X. P. Zhang, and D. Androutsos, "Color image watermarking using multidimensional Fourier transforms," IEEE Trans. Inf. Forensics Security **3** (1), 16–28 (2008).
4. Y. Xu, L. C. Yu, H. T Xu, H. Zhang, and T. Nguyen, "Vector sparse representation of color image using quaternion matrix analysis," IEEE Trans. Image Processing **24** (4), 1315–1329 (2015).
5. Z. Wang and A. C. Bovik, "Modern image quality assessment," Synth. Lectures Image, Video, Multimedia Process. **2** (1), 1–156 (2006).
6. F. Ahmed, M. Siyal, and V. U. Abbas, "A secure and robust hash-based scheme for image authentication," Signal Process. **90** (5), 1456–1470 (2010).
7. D. S. Alexiadis and G. D. Sergiadis, "Estimation of motions in color image sequences using hypercomplex Fourier transforms," IEEE Trans. Image Process. **18** (1), 168–187 (2009).
8. F. N. Lang, J. L. Zhou, S. Cang, H. Yu, and Z. Shang, "A self-adaptive image normalization and quaternion PCA based color image watermarking algorithm," Expert Syst. Appl. **39** (15), 12046–12060 (2012).
9. B. J. Chen, G. Coatrieux, G. Chen, X. M. Sun, J. L. Coatrieux, and H. Z. Shu, "Full 4D quaternion discrete Fourier transform based watermarking for color images," Digit. Signal Process. **28** (1), 106–119 (2014).
10. Z. H. Shao, H. Z. Shu, J. S. Wu, B. J. Chen, and J. L. Coatrieux, "Quaternion Bessel-fourier moments and their invariant descriptors for object reconstruction and recognition," Pattern Recogn. **47** (2), 603–611 (2014).
11. O. N. Subakan and B. C. Vemuri, "A quaternion framework for color image smoothing and segmentation," Int. J. Comput. Vision **91** (3), 233–250 (2011).
12. W. R. Hamilton, *Elements of Quaternions* (Longmans Green, London, 1866).
13. T. A. Ell, and S.J. Sangwine, "Hypercomplex Fourier transforms of color images," IEEE Trans. Image Process. **16** (1), 22–35 (2007).
14. S. J. Sangwine and T. A. Ell, "Hypercomplex Fourier transforms of colour images," in *Proc. IEEE Int. Conf. on Image Processing (ICIP 2001)* (Thessaloniki, 2001), pp. 137–140.
15. N. Le Bihan and S.J. Sangwine, "Quaternion principal component analysis of colour images," in *Proc. IEEE Int. Conf. on Image Processing (ICIP)* (Barcelona, 2003), pp. 809–812.
16. S. Sangwine and T. A. Ell, "The discrete Fourier transform of a colour image," in *Image Processing II: Mathematical Methods, Algorithms and Applications,* Ed. by J. M. Blackledge and M. J. Turner (Horwood Publ., 2000), pp.430–441.
17. T. A. Ell, "Hypercomplex spectral transforms," Ph.D. Dissertation (Univ. Minnesota, Minneapolis, 1992).
18. C. E. Moxey, S. J. Sangwine, and T. A. Ell, "Color-grayscale image registration using hypercomplex phase correlation," in *Proc. IEEE Int. Conf. on Image Processing (ICIP)* (Rochester, 2002), pp. 385–388.
19. W. L. Chan, H. Choi, and R. G. Baraniuk, "Coherent multiscale image processing using dual-tree quaternion wavelets," IEEE Trans. Image Process. **17** (7), 1069–1082 (2008).
20. W. L. Chan, H. Choi, and G. Baraniuk, "Directional hypercomplex wavelets for multidimensional signal analysis and processing," in *Proc. IEEE Int. Conf. Acoustics, Speech and Signal Processing (ICASSP 2004)* (Montreal, 2004), pp. 996–999.
21. T. Batard, M. Berthier, and C. Saint-Jean, "Clifford-Fourier transform for color image processing," in *Geometric Algebra Computing* (Springer, London, 2010), pp. 135–162.
22. Y. N. Li, "Quaternion polar harmonic transforms for color images," IEEE Signal Process. Lett. **20** (8), 803–806 (2013).
23. S. Li, M. C. Lee, and C. M. Pun, "Complex Zernike moment features for shape-based image retrieval," IEEE Trans. Syst. Man Cyb. A **39** (1), 227–237 (2009).
24. A. Kolaman and O. Yadid-Pecht, "Quaternion structural similarity: a new quality index for color images," IEEE Trans. Image Processing **21** (4), 1526–1536 (2012).
25. M. Bober, "MPEG-7 visual shape descriptors," IEEE Trans. Circuits Syst. Video Technol. **11**, 716–719 (2001).

26. S. J. Sangwine, "Fourier transforms of colour images using quaternion or hypercomplex, numbers," Electron. Lett. **32** (21), 1979–1980 (1996).

27. T. A. Ell, *Hypercomplex Spectral Transformations* (Univ. of Minnesota, 1992).

28. W. R. Hamilton, *Elements of Quaternions* (Longmans, Green & Company, 1866).

29. The Moving Picture Experts Group (MPEG). http://www.chiariglione.org/mpeg. Cited Jan. 12, 2009.

30. A. Amanatiadis, V. G. Kaburlasos, A. Gasteratos, and S. E. Papadakis, "Evaluation of shape descriptors for shape-based image retrieval," Image Processing **5**, 493–499 (2011).

31. C. S. Pooja, "An effective image retrieval system using region and contour based features," in *Proc. IJCA Int. Conf. on Recent Advances and Future Trends in Information Technology* (Patiala, 2012), pp. 7–12.

32. K. M. Hosny, "Exact and fast computation of geometric moments for gray level images," Appl. Math. Comput. **189**, 1214–1222 (2007), S. Liao, M. W. Law, and A. Chung, "Dominant local binary patterns for texture classification," IEEE Trans. Image Processing **18** (5), 1107–1118 (2009).

33. C. Y. Wee and R. Paramesran, "On the computational aspects of Zernike moments," Image Vision Comput. **25**, 967–980 (2007).

34. C. Singh and R. Upneja, "Error analysis in the computation of orthogonal rotation invariant moments," J. Math. Imaging Vision **49**, 251–271 (2014).

35. A. Khatabi, A. Tmiri, and A. Serhir, "A novel approach for computing the coefficient of ART descriptor using polar coordinates for gray-level and binary images," in *Advances in Ubiquitous Networking* (Springer, 2016), pp. 391–401.

Abderrahim Khatabi (born 1987) received a master's degree of networks and telecommunications from Chouaib Doukkali University Faculty of Science EI Jadida, Morocco in 2011. He is currently pursuing his Ph.D. degree (Computer Science) at the Chouaib Doukkali University Faculty of Science, Jadida, Morocco. His research interests include Medical Image Processing.

Amal Tmiri is currently a professor in Chouaib Doukkali University Faculty of Science, Department of Computer science, Laboratory LAROSERI, EI Jadida, Morocco. His research interests include Medical Image Processing.

Ahmed Serhir is professor in Chouaib Doukkali University Faculty of Science, Department of Math, Laboratory of Fundamental mathematics, EI Jadida, Morocco. His research interests Algebra and fundamental Mathematics.